



HAL
open science

Peristaltic pumping by huge amplitude piezoelectric traveling wave actuator

François Pigache, Leonard Coutant, Laetitia Pernod, Julien Michel Fontaine

► **To cite this version:**

François Pigache, Leonard Coutant, Laetitia Pernod, Julien Michel Fontaine. Peristaltic pumping by huge amplitude piezoelectric traveling wave actuator. 2021 IEEE International Workshop of Electronics, Control, Measurement, Signals and their application to Mechatronics (ECMSM), Jun 2021, Liberec, France. pp.1-6, 10.1109/ECMSM51310.2021.9468866 . hal-03287172

HAL Id: hal-03287172

<https://ut3-toulouseinp.hal.science/hal-03287172>

Submitted on 15 Jul 2021

HAL is a multi-disciplinary open access archive for the deposit and dissemination of scientific research documents, whether they are published or not. The documents may come from teaching and research institutions in France or abroad, or from public or private research centers.

L'archive ouverte pluridisciplinaire **HAL**, est destinée au dépôt et à la diffusion de documents scientifiques de niveau recherche, publiés ou non, émanant des établissements d'enseignement et de recherche français ou étrangers, des laboratoires publics ou privés.

Peristaltic pumping by huge amplitude piezoelectric traveling wave actuator

François Pigache

Université de Toulouse; INP, UPS ;
LAPLACE; CNRS ; UMR 5213 Toulouse,
France
pigache@laplace.univ-tlse.fr

Léonard Coutant

Université de Toulouse; INP, UPS ;
LAPLACE; CNRS ; UMR 5213 Toulouse,
France
coutant@laplace.univ-tlse.fr

Laetitia Pernod

Institut de Recherche de l'Ecole Navale
(IRENav), EA 3634 - Ecole Navale, Brest,
France
laetitia.pernod@ecole-navale.fr

Julien Michel Fontaine

Université de Toulouse; INP, UPS ;
LAPLACE; CNRS ; UMR 5213 Toulouse,
France
Julien.fontaine@alumni.enseeiht.fr

Abstract -- This article deals with the design and drive of a thin plate wall, bent by piezoelectric fibers (MFC- Macro Fiber Composite). The purpose of this deformable membrane is to drive a moving fluid inside a thin channel according to a principle similar to peristaltic pumping. To promote this pumping effect, the deformation of the wall must be as a traveling wave-like with sufficiently high amplitude to transfer momentum to the fluid.

Keywords— Piezoelectric actuators, peristaltic pumps, flexible electronics.

I. INTRODUCTION

Pumping or micro-pumping of fluids may be achieved using various physical principles, as described in Fig. 1. Moreover, many different technologies are available to realize the pumping, depending on the requirements of the system [1-2]. These technologies may use mechanical elements (or not), flexible membranes, expansion tanks, or electrical and magnetic fields. Focusing on peristaltic pumping, which is the main interest of this work, two reviews of micro-pumps technologies are presented in [3-4].

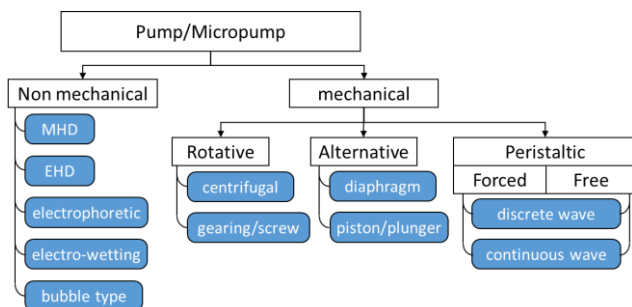


Fig. 1 Comparison of mechanical performances of smart materials [1-2]

In addition, various electroactive materials have been studied in order to meet the specific technical requirements of mechanical solutions (e.g. compactness) and performance of fluid pumps (e.g. desired mass flow rate). They demonstrate various capabilities in terms of stroke, blocked force, and operating frequency. Among these electroactive materials, this article focuses on peristaltic pumping solutions actuated by piezoelectric elements, which may be classified

according to the category of the wave propagated [5]:

1) The traveling wave is said to be *free* (or natural) when one or more actuators create a mechanical wave propagated freely in the membrane in either a plate mode or surface wave [5-6]. Its operation is dynamic and most often resonant;
2) It is said to be a *forced wave* when the drive is distributed so that each deformation profile at every instant can be obtained in quasi-static mode (even if the actuators can be operated at resonance frequency to increase their displacement):

2a) The forced wave will be referred to as *discrete* when the deformation is obtained by the coordinated deformation of a set of actuators, for example in the multi-chamber devices with diaphragms in series [7].

2b) Conversely, the forced wave will be referred to as *continuous* when the actuator has a uniformly distributed contribution associated with a longitudinal movement in the direction of wave propagation (such as conventional peristaltic roller pumps).

Due to the fact that they can be actuated by few actuators and that the wave is naturally propagated, free wave solutions may seem attractive at first sight. However, they have the disadvantage of low amplitude of deformation and they do not allow transferring large momentum to the fluid and consequently, they present a relatively low mass flow rate capability.

The aim of this study is to present the development and successful subsequent testing of a forced wave actuation realized from an electroactive membrane, that is, a flexible material equipped with several piezoelectric ceramics used as actuators. These transducers may be driven separately or together (by sets of several transducers) to produce a deformation with a specific wave shape and propagation law within the membrane. The objective is to maximize the mass flow rate induced by the deformation of the membrane and the associated pumping of fluid. This requires in turn two nested optimization loops: (i) an optimal design of the membrane (i.e. number and location of the piezoelectric transducers) and (ii) an optimal design of the actuation law of the transducers (i.e. voltage, number and configuration of the

sets of transducers). The experimental prototype is first presented, then a pseudo-analytical model of the coupled electromechanical behavior of the electroactive membrane is derived to enable the realization of the optimization loops. Finally, an experimental validation of the pumping capabilities of this peristaltic pumping solution is presented.

II. EXPERIMENTAL PROTOTYPE

The electroactive membrane was specifically designed for this application, and is made of a 110 mm x 80 mm x 750 μm thin plate constituting a deformable substrate on which piezoelectric transducers are glued. These transducers may be driven separately or together (by sets of several transducers referred to as *piezo-segments*), and for this first demonstration of the pumping capabilities, fifteen transducers are used (refer to Fig. 2 and Fig 3). The piezoelectric transducers are *Macro Fiber Composite*TM (MFC) actuators commercialized by Smart Materials and consist of an active layer sandwiched between two encapsulating layers of Pyralux[®] made of Kapton, acrylic and epoxy shells, as illustrated on Fig 3 for a random configuration. These encapsulation layers guaranty a 1500V voltage supply insulation and support the mechanical stress during bending. Overall dimensions of the transducers (including the encapsulating layers) are 5mm x 60mm x 350 μm . All the transducers considered together form an equivalent MFC actuator operating in transverse coupling mode (d_{31} mode).

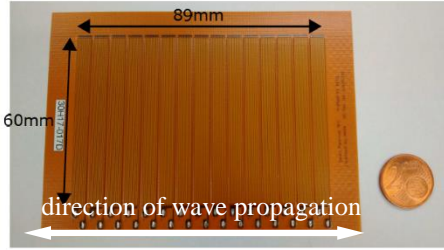


Fig. 2 Custom-made electroactive membrane using MFC actuators

III. PSEUDO ANALYTICAL MODEL

A. Set of assumptions

A pseudo-analytical model of the coupled electrical-mechanical behavior of the electroactive membrane is derived in order to express the mechanical displacement of the bending wall as a function of the voltage supply of the piezo-segments, under the following assumptions:

- 1) Isotropy and homogeneity of each material
- 2) Linear elasticity for each material
- 3) No geometric nonlinearities (“small perturbations”)
- 4) Thin beam theory (Navier-Bernoulli): the thin plate dimensions allow neglecting the following vector components of stress $\bar{\sigma}$ and strain $\bar{\epsilon}$:
 $\sigma_{22} = \sigma_{33} = 0$ and $\epsilon_{31} = \epsilon_{32} = \epsilon_{12} = 0$
- 5) Linear piezoelectricity
- 6) Quasi-static analysis
- 7) Invariant problem in the width direction

The bending behavior of the membrane is numerically solved in free displacement (no external force induced by the

presence of fluid in contact) and as a function of the set of the voltage supply.

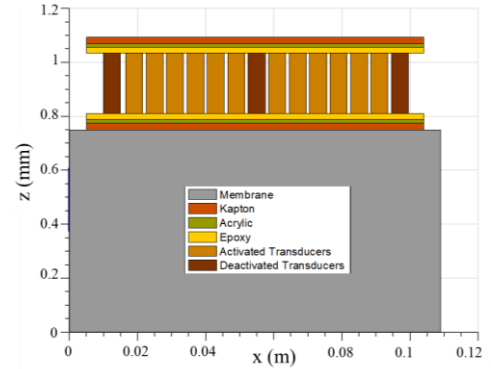


Fig. 3 Dimensions of the deformable wall

B. Governing equations

The governing equations of the problem are the Cauchy equation for the mechanical part

$$\vec{\nabla} \cdot \bar{\sigma} = \vec{0} \quad (1)$$

and the Maxwell-Gauss equation in a dielectric medium for the electrostatic part

$$\vec{\nabla} \cdot \vec{D} = 0 \quad (2)$$

with the assumptions on the piezo-elements

$$D_1 = D_2 = 0 \quad (3)$$

where $\bar{\sigma}$ is the second-order Cauchy stress tensor and \vec{D} the first-order electric displacement field tensor.

C. Closure with constitutive equations

The governing equations (1) and (2) are partially closed using, on the one hand, the constitutive equation of a linear elastic material (Hooke’s law) for the mechanical part, written under assumptions (1)-(4),

$$\sigma_{11} = c_{11}^E \epsilon_{11} \quad (4)$$

and, on the other hand, the constitutive equations for linear piezoelectricity for the electrostatic part, also written under assumptions (1)-(5):

$$\begin{cases} \sigma_{11} = c_{11}^E \epsilon_{11} - e_{31} E_3 \\ D_3 = e_{31} \epsilon_{11} + \epsilon_{33}^{\sigma} E_3 \end{cases} \quad (5)$$

$$(6)$$

where \bar{c} is a fourth-order elasticity tensor, $\bar{\epsilon}$ is the second-order strain tensor, \bar{e} is the third-order piezoelectric tensor and $\bar{\epsilon}^{\sigma}$ is the second-order dielectric permittivity tensor.

D. Closure with gradient relationships

The governing equations (1) and (2) are also closed using the gradient relationship on the strain $\bar{\epsilon}$, written under assumption (1)-(4) for the mechanical part,

$$\epsilon_{11} = u_{1,1} - z \cdot u_{3,11} \quad (7)$$

and the Maxwell-Faraday static equation (*i.e* the electric field is curl-free and thus derive from an electric potential V) for the electrostatic part,

$$E_3 = -V_{,3} \quad (8)$$

where $u_{i,j}$ is the derivative expression of the displacement in (i) direction, derived according to (j).

E. Static equilibrium equations

The composition of the medium is simplified and considered as a set of segments along the length, illustrated in Fig. 4.

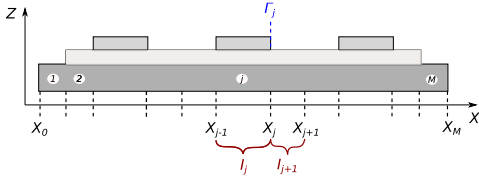


Fig. 4 Discretization of the membrane

The Cauchy equation (1) may be simplified using the static equilibrium of each plane section S_j (at coordinate x) belonging to a segment (J) thanks to the equalities of internal resultant force $\vec{R}_j(x)$ and moment $\vec{M}_{f,j}^P(x)$ at point P as follows:

$$\forall J \in \llbracket 1, M \rrbracket \quad \forall x \in I_j \quad \left\{ \begin{array}{l} \frac{d\vec{R}_j(x)}{dx} + \vec{q}_j(x) = \vec{0} \\ \frac{d\vec{M}_{f,j}^P(x)}{dx} + \vec{x} \wedge \vec{R}_j(x) + \vec{m}_j(x) = \vec{0} \end{array} \right. \quad (9)$$

With $\vec{q}_j(x)$ and $\vec{m}_j(x)$ the distributed forces and moments respectively.

Moreover, the invariant problem in the y -direction leads to only consider the resultant force according to \vec{x} and the moment according to \vec{y} . It finally comes the simplified expression of the resultant force and moment depending on the axial stress σ_{11} and projected on the axis \vec{x} and \vec{y} respectively

$$\vec{R}_j(x) \cdot \vec{x} = \iint_{S_j} \sigma_{11}(x, z) \cdot dydz = N_j(x) \quad (10)$$

$$\vec{M}_{f,j}^P \cdot \vec{y} = \iint_{S_j} z \cdot \sigma_{11}(x, z) \cdot dydz = M_j(x) \quad (11)$$

In addition, it is possible to consider the different layers stacked in the thickness, as shown in Fig. 5. Each layer k may be a passive (no voltage) or an active piezoelectric layer, with distinct material properties. As a consequence, the second term $-e_{31}E_3$ of the right-hand term of (5) only exists for active piezoelectric layers. Let \mathcal{P} be the mathematical set of all active piezoelectric layers of a section J .

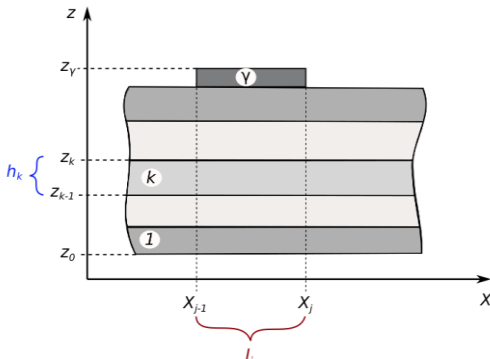


Fig. 5 Multilayer wall thickness and its discretization

From this discretization, the surface of the segment may be expressed as :

$$\iint_{S_j} dydz = \sum_{k=1}^{\gamma} l_k \int_{z_{k-1}}^{z_k} dz$$

with l_k the width of the layer k .

Considering active and passive layers of section J , (10) and (11) yields:

$$\left\{ \begin{array}{l} N_j(x) = \sum_{k=1}^{\gamma} l_k c_k \int_{z_{k-1}}^{z_k} \varepsilon_{11}(x, z) \cdot dz - \sum_{k \in \mathcal{P}} l_k e_k \int_{z_{k-1}}^{z_k} E_3(x, z) \cdot dz \\ M_j(x) = \sum_{k=1}^{\gamma} l_k c_k \int_{z_{k-1}}^{z_k} z \cdot \varepsilon_{11}(x, z) \cdot dz - \sum_{k \in \mathcal{P}} l_k e_k \int_{z_{k-1}}^{z_k} z \cdot E_3(x, z) \cdot dz \end{array} \right.$$

with e_k the piezoelectric coefficient of the k^{th} piezoelectric layer.

Substituting (7) in the couple of equations above, it comes:

$$\sum_{k=1}^{\gamma} l_k c_k \int_{z_{k-1}}^{z_k} \varepsilon_{11}(x, z) \cdot dz = A_j \frac{du_{1,j}(x)}{dx} - B_j \frac{d^2 u_{3,j}(x)}{dx^2}$$

$$\sum_{k=1}^{\gamma} l_k c_k \int_{z_{k-1}}^{z_k} z \cdot \varepsilon_{11}(x, z) \cdot dz = B_j \frac{du_{1,j}(x)}{dx} - D_j \frac{d^2 u_{3,j}(x)}{dx^2}$$

With the respective coefficients

$$A_j = \sum_{k=1}^{\gamma} l_k h_k c_k \quad B_j = \sum_{k=1}^{\gamma} c_k l_k \frac{(z_k^2 - z_{k-1}^2)}{2}$$

$$D_j = \sum_{k=1}^{\gamma} c_k l_k \frac{(z_k^3 - z_{k-1}^3)}{3}$$

The coefficients A_j and D_j correspond to the longitudinal tensile stiffness and flexural stiffness respectively.

The coefficient B_j is associated to the nonsymmetrical property of the membrane according to its thickness. Thus, it associates the longitudinal displacement to the bending moment, and the bending displacement to the normal force. B_j becomes null if the layers are symmetrical on both sides of the median plane.

According to the reasonable assumption of constant and unidirectional electric field $E_3(x, z)$ in a piezo element it comes:

$$\sum_{k \in \mathcal{P}} l_k e_k \int_{z_{k-1}}^{z_k} E_3(x, z) \cdot dz = - \sum_{k \in \mathcal{P}} c_k l_k \cdot dV_k$$

$$\sum_{k \in \mathcal{P}} l_k e_k \int_{z_{k-1}}^{z_k} z \cdot E_3(x, z) \cdot dz = - \sum_{k \in \mathcal{P}} l_k \frac{(z_k + z_{k-1}) e_k}{2} dV_k$$

$$\forall J \in \llbracket 1, M \rrbracket \quad \forall x \in I_j \quad (12)$$

$$\begin{cases} \frac{dN_j(x)}{dx} + \bar{q}_j(x) \cdot \vec{x} = 0 \\ \frac{dM_j(x)}{dx} + \left[\vec{x} \wedge \begin{pmatrix} N_j \\ T_{y,j} \\ T_{z,j} \end{pmatrix} \right] \cdot \vec{y} + \bar{m}_j(x) \cdot \vec{y} = 0 \end{cases}$$

$$\begin{cases} \frac{dN_j(x)}{dx} + r_j = 0 \\ \frac{dM_j(x)}{dx} - T_{z,j} + p_j = 0 \end{cases}$$

Differentiating the second equation (12) and substituting the expressions of $N_j(x)$ and $M_j(x)$, it finally gives:

$$\forall j \in \llbracket 1, M \rrbracket \quad \forall x \in I_j$$

$$\begin{cases} A_j \frac{d^2 u_{1,j}(x)}{dx^2} + r_j = 0 \\ -D_j \frac{d^4 u_{3,j}(x)}{dx^4} - \frac{dT_{z,j}}{dx} + \frac{dp_j}{dx} = 0 \end{cases} \quad (13)$$

F. Relations of continuity between segments and boundary conditions

Every segment I_j must satisfy the relations of continuity with the adjacent segment I_{j+1} as follows

$$\forall j \in \llbracket 1, M \rrbracket \quad \forall x \in I_j, \begin{cases} u_{3,j}(x_j) = u_{3,j+1}(x_j) \\ \theta_{2,j}(x_j) = \theta_{2,j+1}(x_j) \\ M_j(x_j) = M_{j+1}(x_j) \\ T_{3,j}(x_j) = T_{3,j+1}(x_j) \end{cases}$$

with $\theta_{2,j}$ and $T_{3,j}$ the angular displacement according y and the normal force according z respectively.

At the boundary coordinates along x (x_0 and x_M), the bending wall is mechanically maintained fixed. The membrane can be fixed according to different boundary conditions, i.e. clamped or supported.

The vertical displacement u_3 is null at x_0 and x_M

$$\begin{cases} u_{3,1}(x_0) = 0 \\ u_{3,M-1}(x_M) = 0 \end{cases}$$

If the ends of the wall are supported, the bending moments are null

$$\begin{cases} M_1(x_0) = 0 \\ M_{M-1}(x_M) = 0 \end{cases}$$

While if the ends of the wall are clamped, the angular displacements are null

$$\begin{cases} \theta_{2,1}(x_0) = 0 \\ \theta_{2,M-1}(x_M) = 0 \end{cases}$$

The complete set of equations is finally solved numerically using Matlab® with a discretization along x and by respecting the relations of continuity and boundary conditions. The results are illustrated for a custom voltage supply of the 15 segments, presented in Fig. 6. The Fig. 6.a shows the multiple layers composing the membrane.

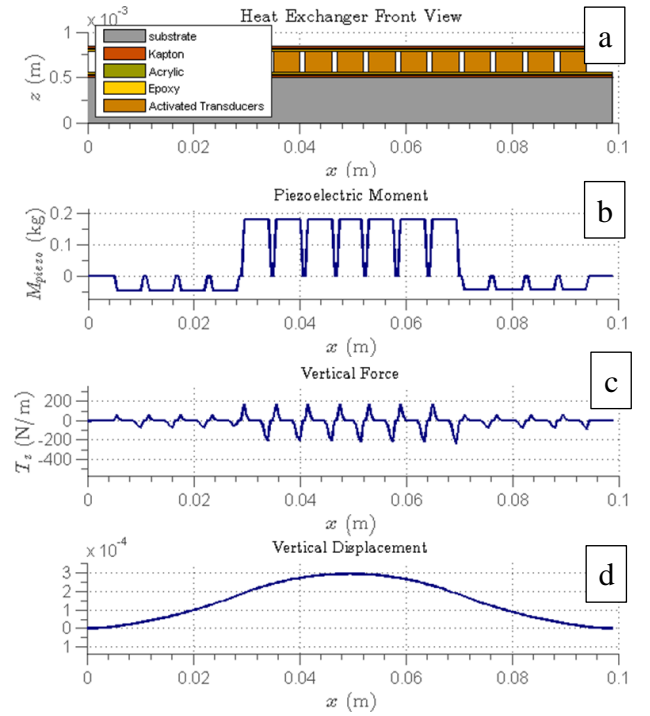


Fig. 6 Vertical displacement of the wall for a specific voltage distribution

The voltage distribution is illustrated by the resulting piezoelectric moment in Figure 7.b. Then, the vertical force distribution $T_z(x)$ and finally the corresponding vertical displacement are given.

This theoretical displacement of the membrane is obtained for a static voltage supply. The dynamic bending is obtained by successive static steps if the frequency is sufficiently low. The next step consists of appropriately supplying the wall to generate a travelling wave-like displacement in x direction. This oriented wave movement is expected to promote the transfer momentum to the fluid.

IV. GENERATION OF THE TRAVELLING WAVE

A. Definition of the set of voltage supply signals

As mentioned in introduction, the objective is now to derive the optimal voltage supply law to maximize the mass flow rate. From preliminary studies, a deformation of the membrane as a travelling wave is expected to be the optimal waveform to enhance the transfer momentum to the fluid. However, several technical requirements prevent the generation of an ideal travelling wave: (i) the edges of the membrane must be clamped, (ii) the wavelength must be roughly a centimeter long in a finite flat domain and (iii) due to different tensile strengths in compression and tension the MFC transducers require a non-symmetrical voltage supply. Consequently, to promote a preferred direction of propagation of the pseudo-travelling wave, an appropriate sequence of voltage supply must be defined so that the deformation of the membrane will fit as much as possible to a natural travelling wave. For this purpose, an optimization procedure is used from Matlab® *pattern search* function. This results in a set of nontrivial voltage waveforms giving a good control of the wave shape at every time step.

B. Experimental validation of the membrane displacement model

The model of the mechanical displacement of the membrane is experimentally validated, using a test bench specifically developed to:

- 1) Supply the piezoelectric segments with various and custom voltage waveforms,
- 2) Map the resulting deformation of the membrane,
- 3) Monitor the entire test bench from a computer.

In order to measure the vertical displacement of multiple points on the deformed surface, a class 2 laser sensor LK-H052 (spot diameter of $50 \mu\text{m}$, Resolution $0.025 \mu\text{m}$) is mounted on an XY-table. The 15 piezoelectric segments are driven with a four channels linear amplifier with a range of -500 V up to $+1500 \text{ V}$. The limited number of voltage channels implies to wisely group subsets of piezo segments.

The input voltage of the linear amplifier, the drive of the XY-table positioning, and the data acquisition are fully managed from a computer with Matlab@Simulink programme associated with a OPAL-RT OP4510 real-time simulator equipped with multiple analog and digital Inputs/Outputs (I/O).

The test bench is briefly described by the scheme on Fig. 7.

A slight discrepancy observed along the width is induced by the necessary wires and welding of piezo segments. Nevertheless, a good accuracy is observed between the experimental average displacement along x in Fig. 8.b compared to the model in Fig. 8.a.

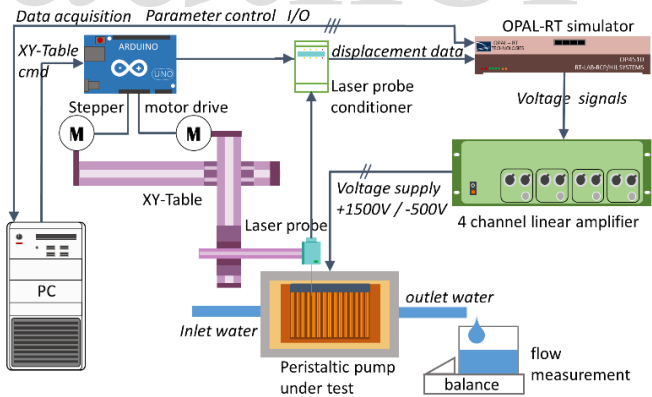


Fig. 7 Scheme of the complete test bench

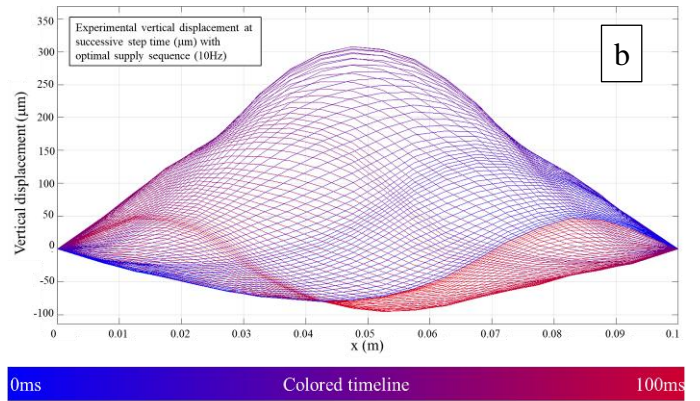
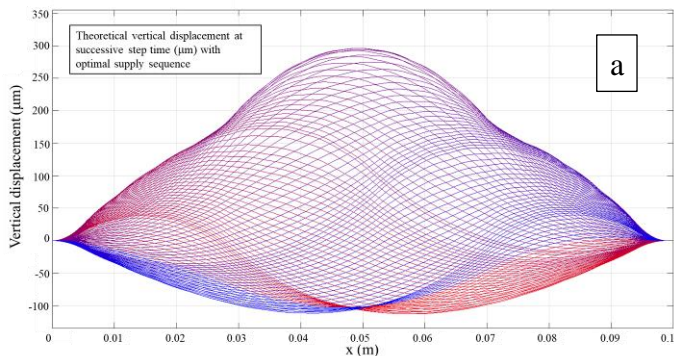


Fig. 8 Membrane wave shapes at successive step time during a full electrical period (a) theoretical (b) experimental

C. Evaluation of mass flow capability

After validating the membrane model and the experimental test bench, the mass flow rate is estimated without considering the fluid-structure interaction (no effect of the fluid on the mechanical). This flow rate is estimated considering an ideal water (no viscosity) which can be an acceptable assumption at low operating frequency. Thus, an iterative algorithm [8] is used to evaluate the mass flow depending on the periodic membrane deformation. It consists of respecting the volume conservation at every step of the wave change and evaluating the mass flow (through the outlet) and reverse mass flow (through the inlet). The Fig. 9 illustrates the theoretical pump.

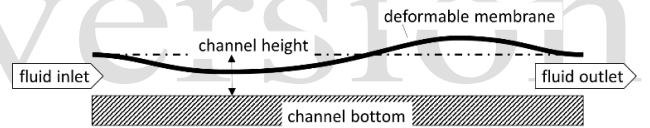


Fig. 9 Description of the peristaltic pump

The deformable membrane is clamped on its edges by respecting a distance with the bottom of the channel. Because the fluid is considered as ideal, the mass flow is theoretically proportional to the frequency of the periodic deformation. Preliminary investigation consists in estimating the mass flow of water at 1Hz in function of the height of the channel. The selected deformation sequence is the one given in Fig. 8.a. This parametric study gives the results in Fig. 10. It is calculated from $100 \mu\text{m}$ of the height channel which corresponds to the wave shape amplitude under the neutral position.

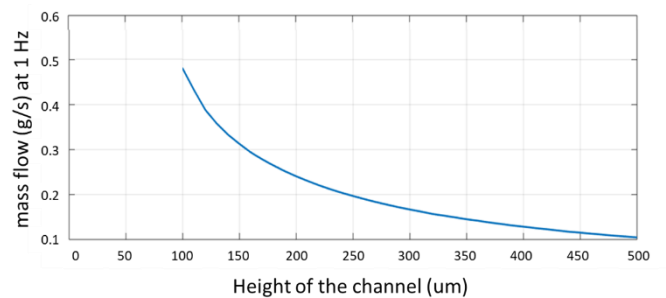


Fig. 10 Mass flow at 1Hz in function of the height of channel

The algorithm is not able to take into account the contact

of the membrane with the channel bottom and it will be extended in future. The results show a nonlinear and decreasing relation of the mass flow with the height of the channel. This trend is explained by the fact that the larger the height, the less the capability to promote the fluid movement in a direction. The maximal mass flow is less than 1g/s for 1 Hz. Even if the real fluid behavior implies losses with the increasing of the frequency, it is reasonable to consider that the mass flow can be significantly increased with this latter.

V. CONCLUSION

This paper presents the preliminary model and development of a peristaltic pump relying on a deformable membrane actuated by MFC piezoelectric actuators. Its main interest consists in its very compact design. A pseudo-analytical model of the coupled electromechanical behavior of the electroactive membrane is first derived in order to design the optimal voltage supply law. Indeed, the piezoelectric actuators must be driven with a specific voltage law to generate a deformation of the membrane similar to a travelling wave with a significant amplitude, high enough to realize a flat peristaltic pump and maximize the mass flow rate. Then, the experimental measurements of the electroactive membrane in deformation have demonstrated a satisfactory accuracy with the theoretical predictions in free displacement, up to 300 μm of maximal flexion amplitude at 1Hz. Moreover, preliminary pumping capabilities are promising. Nevertheless, the theoretical results need to be consolidated by simulations taking into account the dynamic

properties of the moving fluid and its interaction with the deformable structure. Beyond the pumping application, it obviously appears possible to use this deformable membrane as a morphing surface, inchworm actuator, powder transport or many other applications.

REFERENCES

- [1] D. J. Laser, J. G. Santiago. "A review of micropumps", *Journal of micromechanics and microengineering*, 14(6), R35–R64, 2004.
- [2] A. Nisar, N. Afzulpurkar, B. Mahaisvariya, and A. Tuantranont, "Mems-based micropumps in drug delivery and biomedical applications", *Sensors and Actuators B, Chemical*, 130(2), p. 917–942, 2008.
- [3] Farzad Forouzandeh, Arpys Arevalo, Ahmed Alfadhel, David A. Borkholder: "A review of peristaltic micropumps", *Sensors and Actuators A* 326 (2021) 112602
- [4] B. Husband, M. Bu, A. GR Evans, T. Melvin. "Investigation for the operation of an integrated peristaltic micropump", *Journal of Micromechanics and Microengineering*, 14(9), S64-S69, 2004.
- [5] C. Hernandez, Y. Bernard, and A. Razek. "Design and manufacturing of a piezoelectric traveling-wave pumping device", *IEEE trans. on ultrasonics, ferroelectrics, and frequency control*, 60(9), p. 1949–1956, 2013.
- [6] J-H Oh, K-J Lim, J-H Yoon, S-H Cho, H-H Kim, "Fabrication and characteristics of ring type valveless piezoelectric micro-pump using peristaltic motion", *Integrated Ferroelectrics*, 114(1), 49–58, 2010.
- [7] J. M. Fontaine, F. Pigache, M. Miscevic, F. Topin, J-F. Rouchon, "Investigations in actuator solutions for active cooling in embedded systems", *Physical and Chemical Phenomena in Heat Exchangers and Multifunctional Reactors for Sustainable Technology Eurotherm Seminar*, 106, 10-11 Oct 2016 Paris
- [8] J. M. Fontaine, F. Pigache, M. Miscevic, J. Rouchon and F. Topin, "Studying impacts of travelling wave shape on pumping for active cooling", *2017 IEEE International Workshop of Electronics, Control, Measurement, Signals and their Application to Mechatronics (ECMSM)*, pp. 1-6, 2017.

author version